JOURNAL OF GUIDANCE, CONTROL, AND DYNAMICS
Vol. 30, No. 2, March–April 2007

Engineering Notes

ENGINEERING NOTES are short manuscripts describing new developments or important results of a preliminary nature. These Notes should not exceed 2500 words (where a figure or table counts as 200 words). Following informal review by the Editors, they may be published within a few months of the date of receipt. Style requirements are the same as for regular contributions (see inside back cover).

Optimal Path Planning with a Kinematic Airplane Model

Timothy G. McGee*
Johns Hopkins University Applied Physics Laboratory, Laurel, Maryland 20723
and
J. Karl Hedrick†
University of California, Berkeley, California 94720

DOI: 10.2514/1.25042

Introduction

OPTIMAL path planning is an important problem for robotics and unmanned vehicles. This note describes a method for finding the minimum-time path from an initial position and orientation to a final position and orientation in the two-dimensional plane for an airplane with a bounded turning rate in the presence of a constant wind [1]. This problem was first solved in the no-wind case by Dubins using geometric arguments [2]. Reeds and Shepp extended this result for a vehicle that could reverse its direction [3]. Boissonnat et al. later reproduced the Dubins and Reeds–Shepp results using optimal control methods [4]. These results have also been used for higher-level path planning through multiple points [5,6] and to travel around obstacles [7,8].

The kinematic model assumes a constant velocity airplane traveling in a known constant wind with a magnitude less than the airplane velocity. The control input of the airplane is the turning rate, which is assumed to be bounded. By normalizing the position of the airplane (x, y) so that the velocity is 1 and defining the orientation ψ with respect to the direction of the wind, the equations of motion can be expressed as

$$\dot{\boldsymbol{x}} = \begin{bmatrix} \dot{x} \\ \dot{y} \\ \dot{\psi} \end{bmatrix} = \begin{bmatrix} \cos\psi + \beta \\ \sin\psi \\ u \end{bmatrix} \tag{1}$$

where u is the commanded turning rate with $|u| < \dot{\psi}_{\max}$, and β is the ratio of the wind and airplane velocities with $|\beta| < 1$. Taking the derivative of Eq. (1), it can be seen that the bound on the turning rate is equivalent to an acceleration bound in the ground frame:

$$\sqrt{\ddot{x}^2 + \ddot{y}^2} = \dot{\psi} \tag{2}$$

The goal of the optimization problem is to find the minimum-time path from $\boldsymbol{x}_i = (x_i, y_i, \psi_i)$ to $\boldsymbol{x}_f = (x_f, y_f, \psi_f)$.

The preceding problem statement is equivalent to finding the minimum-time path from an initial position and orientation to a final orientation over a moving virtual target, where the velocity of the virtual target is equal and opposite to the velocity of the wind. The path of the airplane in this redefined problem is its path with respect to the moving "air frame" and will be referred to as the "air path." If this path is flown in the presence of wind, the path of the airplane with respect to the ground will be known as the "ground path." The equations of motion for the airplane in the redefined problem become

$$\dot{\boldsymbol{x}} = \boldsymbol{f}(x, u) = \begin{bmatrix} \cos\psi \\ \sin\psi \\ u \end{bmatrix} \tag{3}$$

The position of the virtual target $\boldsymbol{x}_d$ can be calculated as

$$\boldsymbol{x}_d(t) = \begin{bmatrix} x_f - \beta t \\ y_f \\ \psi_f \end{bmatrix} \tag{4}$$

Given an initial airplane position, $\boldsymbol{x}(0) = \boldsymbol{x}_i$, and an initial virtual target position, $\boldsymbol{x}_d(0) = \boldsymbol{x}_f$, the goal of the redefined problem is to find the input such that $\boldsymbol{x}(T) = \boldsymbol{x}_d(T)$ for the minimum value of T.

Minimum Principle

Following the work of Boissonnat et al. [4], a better understanding of the problem can be gained through the application of optimal control theory. Using the notation of Bryson and Ho [9], we first define the performance index J, which is equal to the intercept time T:

$$J = \int_0^T L \, \mathrm{d}t = \int_0^T 1 \, \mathrm{d}t = T \tag{5}$$

To enforce the maximum turning rate of the vehicle, the dynamics of Eq. (3) are adjoined to the performance index with a multiplier λ, to form the Hamiltonian H:

$$H = L + \lambda^T \boldsymbol{f} = 1 + \lambda_1 \cos\psi + \lambda_2 \sin\psi + \lambda_3 u \tag{6}$$

where the dynamics of the multiplier satisfy

$$\dot{\lambda} = -\frac{\mathrm{d}H}{\mathrm{d}\boldsymbol{x}} = -\begin{bmatrix} 0 & 0 & 0 \\ 0 & 0 & 0 \\ -\sin\psi & \cos\psi & 0 \end{bmatrix} \tag{7}$$

By defining the Hamiltonian and multiplier dynamics in this way, the minimum principle requires that on the optimal trajectory $(\boldsymbol{x}^*, \lambda^*)$, the optimal control u^* must minimize H over the set of all possible inputs u_a at each instance in time:

$$H(\boldsymbol{x}^*, u^*, \lambda^*, t) \le H(\boldsymbol{x}^*, u, \lambda^*, t) \quad \forall\ u \in u_a, \qquad t \in [0, T] \tag{8}$$

Because λ_1 and λ_2 are constant as shown in Eq. (7), satisfying the condition in Eq. (8) is equivalent to satisfying

$$\lambda_3 u^* \le \lambda_3 u \quad \forall\ |u| \le \dot{\psi}_{\max} \tag{9}$$

Presented as Paper 6186 at the AIAA Guidance, Navigation, and Control Conference and Exhibit, San Francisco, 15–18 August 2005; received 8 May 2006; revision received 28 November 2006; accepted for publication 9 October 2006.

*Senior Professional Staff; timothy.mcgee@jhuapl.edu.
†Professor, Department of Mechanical Engineering; khedrick@me.berkeley.edu.

The necessary condition of Eq. (9) allows several properties of the optimal path to be proven:

Property 1: The optimal path consists of maximum-rate turns and straight lines.

Proof: Because λ_1 and λ_2 are constants, $\dot{\lambda}_3$ is equal to zero only for a specific orientation ψ_c, which satisfies $\sin\psi_c\lambda_1 = \cos\psi_c\lambda_2$. Thus, during any nonzero time interval, λ_3 is constant if and only if the airplane travels in a straight line in the air frame parallel to the characteristic direction, ψ_c. Now, the optimality condition in Eq. (9) allows only three input values, dictated by the value of λ_3: on any segment where $\lambda_3 > 0$, $u^* = -\dot{\psi}_{\max}$; on any segment where $\lambda_3 < 0$, $u^* = \dot{\psi}_{\max}$; on any segment where $\lambda_3 = 0$, the airplane must travel in a straight line, implying $u^* = 0$.

Property 2: All straight segments and changes in turning direction on the optimal path must occur on a single line in the air frame.

Proof: As shown by Boissonnat et al. [4], using $\dot{x} = \cos\psi$ and $\dot{y} = \sin\psi$, the equation for $\dot{\lambda}_3$ becomes $\dot{\lambda}_3 = \dot{y}\lambda_1 - \dot{x}\lambda_2$, which integrates to

$$c = \lambda_3 + x\lambda_2 - y\lambda_1 \tag{10}$$

where c is a constant. Because the values of c, λ_1, and λ_2 are constant, each value of λ_3 defines a line parallel to the characteristic direction. The line defined by $\lambda_3 = 0$ is the line on which all switching and straight-line travel must occur.

From Property 2, the optimal path in the air frame must be a chain of circles of radius $R_{\min}$, where $R_{\min}$ is the minimum turning radius in the air frame, that are all tangent along a single switching line. The interior circles in this chain can either have arc lengths less than, greater than, or equal to π as illustrated in Fig. 1. For interior circles with arc lengths less than π, the path length decreases as the number of circles increases and the path becomes a straight line. For interior circles with arc lengths greater than π, the path length decreases as the number of interior circles decreases.

Analysis of the Rendezvous Problem

Using the redefined problem statement, the airplane must rendezvous with a virtual target that travels in a straight line. Any point along this line can be expressed by a single variable d, which is the distance to the virtual target's initial position. Let the function $T_a(d)$ be the minimum time it takes the airplane to travel from its initial position and orientation to the desired orientation at point d. Let $T_{\text{vt}}(d)$ be the time it takes the virtual target to move to point d. The goal of the optimization problem is to find the smallest d at which $T_a(d) = T_{\text{vt}}(d)$. This approach is very similar to that used by Croft et al. to calculate the rendezvous of a manipulator with moving objects [10].

The function $T_a(d)$ can be generated by calculating the length of each of the admissible Dubins path types to point d and letting $T_a(d)$ equal the minimum of these lengths divided by the airplane velocity.

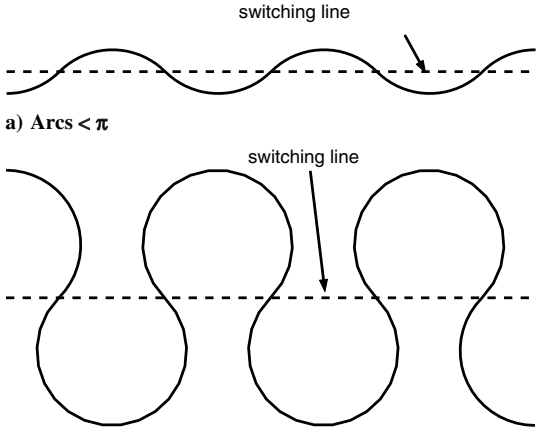

Fig. 1 Illustration of switching line.

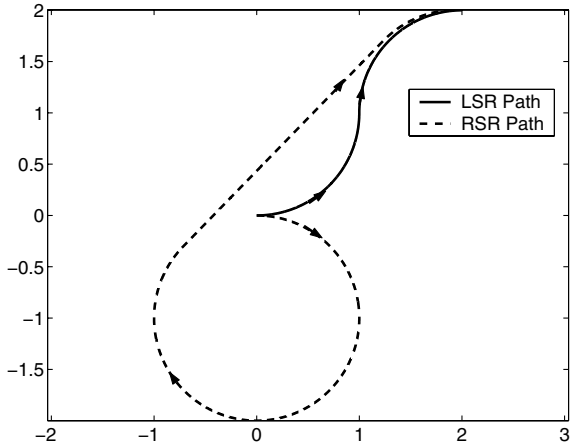

Fig. 2 Discontinuity in optimal path length for small change in final position.

The six admissible Dubins path types are *RSR*, *LSL*, *RSL*, *LSR*, RL_vR, and LR_vL, where R denotes a maximum-rate right turn, L denotes a maximum-rate left turn, S denotes a straight line, and for any three-turn path, the arc length of the center turn, v, is greater than π. It should be noted that the *RSL*, *LSR*, RL_vR, and LR_vL path types cannot be constructed for all boundary conditions. Let the function $\Delta T_{\min}(d)$ be the difference of $T_a(d)$ and $T_{\text{vt}}(d)$:

$$\Delta T_{\min}(d) \stackrel{\text{def}}{=} T_a(d) - T_{\text{vt}}(d) \tag{11}$$

Several important properties of the function $\Delta T_{\min}(d)$ can be proven:

Property 3: $\Delta T_{\min}(d)$ is piecewise continuous, and all discontinuities occur when the *RSL* and *LSR* paths fail to exist.

Proof: It was shown by Bui et al. [11] that the length of the optimal Dubins path is piecewise continuous for changes in the boundary conditions, and that discontinuities occur when the *RSL* and *LSR* paths fail to exist, as shown in Fig. 2. Because the virtual target follows a continuous path, the difference of $T_a(d)$ and $T_{\text{vt}}(d)$ must also be piecewise continuous.

Property 4: $\Delta T_{\min}(d) > 0$ and $\lim_{d\to\infty}\Delta T_{\min}(d) < 0$.

Proof: $T_{vt}(0) = 0$ because the virtual target starts at point $d = 0$, and $T_a(0) > 0$ because the airplane requires some finite time to travel to any point different from its own starting point. Thus $\Delta T_{\min}(0) > 0$. As d approaches ∞, the majority of the airplane path is a straight line that is nearly parallel to the virtual target path. Because $|\beta| < 1$, if d is made large enough, the airplane will always reach point d before the virtual target, making $\Delta T_{\min}(d) < 0$.

Given Property 4, it is clear that $\Delta T_{\min}(d)$ must either equal zero or have a discontinuity across zero for at least one value of d. For given boundary conditions, the resulting $\Delta T_{\min}(d)$ function can thus be classified as one of two types:

Type 1: All $\Delta T_{\min}(d)$ functions such that $\Delta T_{\min}(d) = 0$ at some $d = d^*$, and $\Delta T_{\min}(d) > 0$ for all $d < d^*$.

Type 2: All $\Delta T_{\min}(d)$ functions that are not of Type 1.

Examples of Types 1 and 2 are shown in Figs. 3 and 4, respectively. More properties of the optimal solution can be proven from these path types.

Property 5: For any $\Delta T_{\min}(d)$ function of Type 1, the point d^* is the first point at which the airplane can intercept the virtual target at the specified final orientation.

Proof: By the definition of Type 1, $\Delta T_{\min}(d) > 0$ for all $d < d^*$. Thus the virtual target will always reach any point $d < d^*$ before the airplane.

Property 6: For some boundary conditions, the airplane must travel a non-minimum-distance air path to intercept the virtual target.

Proof: The $\Delta T_{\min}(d)$ function is calculated using the airplane's minimum-distance air path to each point d. If a function of Type 2 is never equal to zero, the airplane can never intercept the virtual target by traveling a minimum-distance air path.

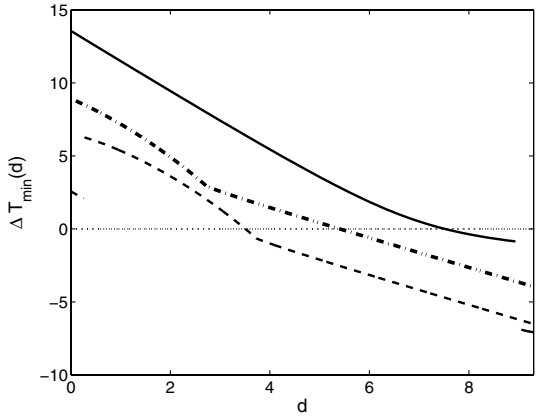

Fig. 3 Examples of $\Delta T_{\min}(d)$ functions of Type 1.

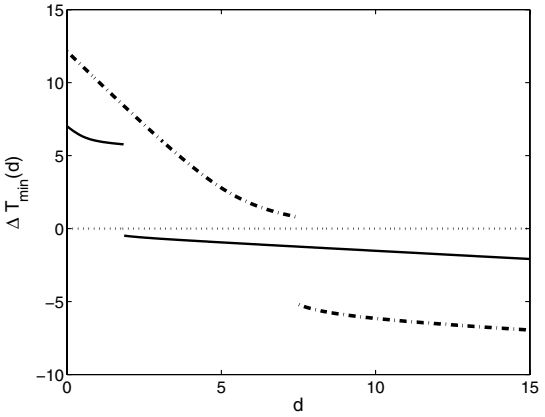

Fig. 4 Examples of $\Delta T_{\min}(d)$ functions of Type 2.

Property 6 implies that for some boundary conditions the airplane must lengthen its air path to allow the virtual target to catch up. From Properties 1 and 2, the airplane must travel maximum-rate turns or straight lines, and all direction changes must occur on a single line in the air frame. Thus, the first option to lengthen the airplane's air path is to use one of the non-minimum-distance Dubins paths. The second option is to lengthen the *RSL* or *LSR* path that caused the discontinuity in $\Delta T_{\min}(d)$ by introducing a path that is a chain of turns where the interior turns are less than π as shown in Fig. 1. Because paths of this type lengthen as the number of interior turns decreases, the longest path of this type contains a single interior turn. Thus, let RL_uR and LR_uL denote paths with a single interior turn whose arc length u is less than π. To further analyze the problem with the addition of these two extra path types, let $\Delta T_X(d)$ define a family of functions:

$$\Delta T_X(d) \stackrel{\text{def}}{=} T_{Xa}(d) - T_{\text{vt}}(d) \tag{12}$$

where X denotes the type of path, including the six Dubins paths (*RSR*, *RSL*, etc.) and the additional RL_uR and LR_uL paths, and $T_{Xa}(d)$ denotes the time required for the airplane to travel to a specific point d using that specific path type. Because each path type is constructed with circles and straight lines in the air frame, their lengths can be easily calculated analytically. It is important to note that not all eight of the $\Delta T_X(d)$ functions are defined for every value of d.

Property 7: For a $\Delta T_{\min}(d)$ function of Type 2, there will be either a RL_vR, LR_vL, RL_uR, or LR_uL path that intercepts the virtual target.

Proof: Consider the case where the discontinuity across zero occurs when the *LSR* path comes into existence. Before the discontinuity, $\Delta T_{LR_vL}(d) > 0$ because $\Delta T_{\min}(d) > 0$ and $\Delta T_{LRvL}(d) \geq \Delta T_{\min}(d)$. Immediately after the discontinuity, $\Delta T_{LRuL}(d) < 0$ because the LR_uL path is equivalent to the *LSR* path. This occurs because the length of the second left arc in the LR_uL path is equal to zero, and the straight portion of the *LSR* path is equal to zero. This leaves two *LR* paths that are equivalent. As d increases, the centers of the two outer turns in the LR_vL and LR_uL curves move further apart. When the centers of the two outer turns are exactly $4R_{\min}$ apart, the LR_vL and LR_uL curves are equivalent, and the arc length of the center curve is π. Because $\Delta T_{LRvL}(d) > 0$ and $\Delta T_{LRuL}(d) < 0$ at the discontinuity and they converge to the same value, one of them must cross zero.

Theorem 1: The optimal path from $\boldsymbol{x}_i$ to $\boldsymbol{x}_f$ for a airplane with a minimum turning radius in the presence of a constant wind will be one of the following set of curves $\{RSR, LSL, RSL, LSR, R L_vR, LR_vL, RL_uR, LR_uL\}$, where $v \geq \pi$ and $u < \pi$.

Proof: It was shown using optimal control methods that the optimal path consists of maximum-rate turns and straight lines. It was also shown that for boundary conditions that produce Type 1 $\Delta T_{\min}(d)$ functions, the optimal path is one of the standard Dubins paths. For Type 2 $\Delta T_{\min}(d)$ functions, the discontinuity occurs when either a *RSL* or *LSR* comes into existence, producing a change of length of less than $2\pi R_{\min}$ in the airplane's air path. The optimal rendezvous point with the virtual target will be found by either using the shortest path that does not cause a discontinuity, which is one of the non-minimum-length Dubins paths, or by lengthening the *RSL* or *LSR* path that produced the discontinuity. The most that a *RSL* or *LSR* path can be lengthened without increasing the length of the curve more than $2\pi R_{\min}$ is to use a LR_uL or RL_uR path. Finally, Property 7 guarantees that one of these types of curves will always intercept the virtual target.

Construction of Optimal Path

To construct the optimal path, a $\Delta T_X(d)$ function can be created for each of the eight admissible path types. For each of these functions, the minimum d^* value where that function is equal to zero is calculated. This can be done using a standard numeric root finding method such as a bisection algorithm or the Newton–Raphson method. The optimal path is chosen as the one that produces the smallest value for d^*.

For completeness, it should be noted that in the presence of wind, it is possible for the optimal path to consist of a turn of exactly 2π and a straight line. These path types are optimal for only a small set of boundary conditions where the initial and final orientations must be identical. To avoid checking for the optimality of these path types, a negligible random amount can be added to the final orientation angle if it is ever exactly equal to the initial orientation angle. This will cause any possible path with a turn of exactly 2π path to become a *RSR* or *LSL* path.

Examples

Several examples of optimal paths in the presence of wind, assuming a maximum turn rate of 1 rad/s, are shown in Figs. 5–8. For Fig. 5, $\boldsymbol{x}_i = (0, 0, \pi/2)$, $\boldsymbol{x}_f = (4, 0, -3\pi/4)$, and $\beta = 0.3$. For Fig. 6, $\boldsymbol{x}_i = (0, 0, \pi/4)$, $\boldsymbol{x}_f = (5, 1, \pi)$, and $\beta = 0.5$. In these first two examples, the optimal rendezvous paths are *RSR* and *LSR*,

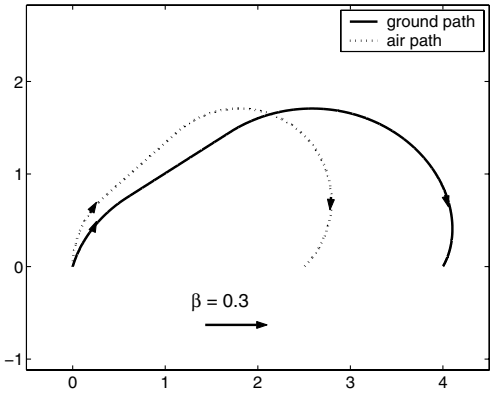

Fig. 5 Example of optimal *RSR* path.

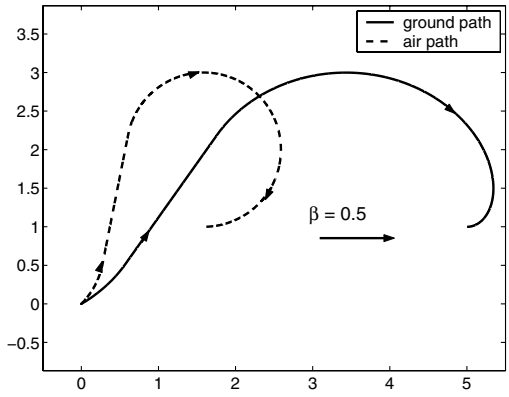

Fig. 6 Example of optimal *LSR* path.

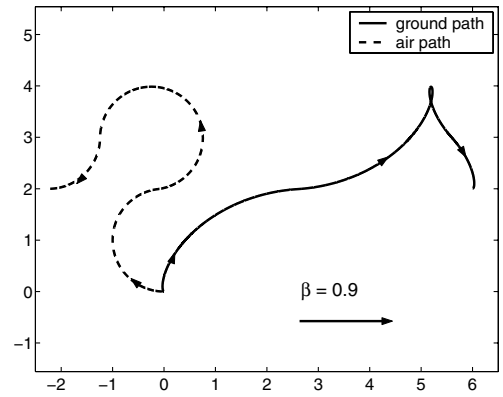

Fig. 7 Example of optimal RL_vR path.

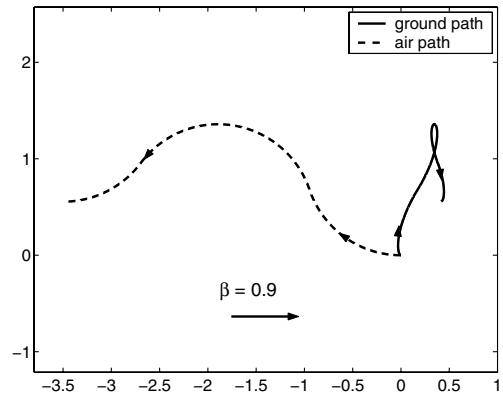

Fig. 8 Example of optimal RL_uR path.

respectively, and represent cases that produce Type 1 $\Delta T_{\min}(d)$ functions. The second two examples illustrate boundary conditions that produce Type 2 $\Delta T_{\min}(d)$ functions. For Fig. 7, $\boldsymbol{x}_i = (0, 0, \pi)$, $\boldsymbol{x}_f = (6, 2, \pi)$, $\beta = 0.9$, and the rendezvous path is a RL_vR path that is a non-minimum-length Dubins path. For Fig. 8, $\boldsymbol{x}_i = (0, 0, \pi)$, $\boldsymbol{x}_f = (0.43, 0.56, \pi)$, $\beta = 0.9$ and the path is of type RL_uR.

Practical Applications

Although the described analysis assumes an idealized model, several minor extensions and modifications could allow it to be used as part of a practical path-planning algorithm. First, the defined problem only calculates a path between two points with given orientations. A more realistic problem would be to design a minimum-time path over several ground points. For this problem, the preceding result could be used to calculate an optimal path through an ordered set of points by minimizing the total path time over the vector of orientation angles at each point [5,12]. Second, the model assumes a known constant wind. In an actual setting, the wind would never be exactly known or constant, although a reasonable estimate with known uncertainty bounds could be available. In this case, a reference ground path could be calculated assuming a turning rate bound that is less than the actual maximum turning rate. The airplane could then track this reference path in the presence of uncertainty [12]. Third, in many airplane applications there are sensor constraints such as a fixed forward-looking sensor or the need to fly wings level during data collection. This problem has been addressed in the past in the absence of wind by requiring that the airplane travel in a straight line of a given length over the target location [6]. The geometry of this approach can be easily extended to account for wind as illustrated in Fig. 9.

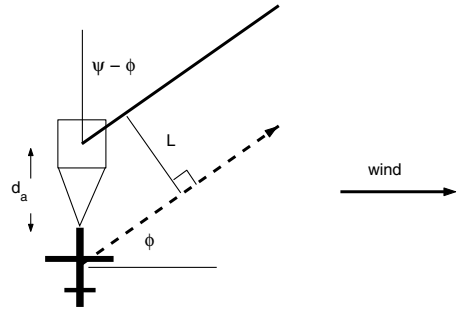

Fig. 9 Geometry of path planning with forward-looking sensor.

For a given airplane orientation ψ, the direction of the airplane ground velocity ϕ can be calculated as

$$\phi = \arctan\left(\frac{\sin\psi}{\cos\psi + \beta}\right) \tag{13}$$

With a forward-looking sensor with a footprint at a fixed distance d_a in front of the airplane, the airplane must travel along a second line offset from the sensor path, where the offset L can be calculated as

$$L = d_a \sin(\psi - \phi) \tag{14}$$

Thus, in the presence of sensor constraints, the result described in this note can be used to calculate paths connecting the endpoints of the linear paths over the target locations.

Conclusions

This note studied the problem of finding the optimal path from an initial position and orientation to a final position and orientation for an airplane with a bounded turning rate in the presence of a constant wind. It was shown that the well-known set of Dubins paths is incomplete in the presence of wind, and a complete set of admissible path types was presented. An iterative method for solving for the optimal path, which redefined the problem using a virtual moving target, was also presented and several extensions of the result for practical path planning were given.

Acknowledgments

This work was done while Timothy G. McGee was a graduate student at the University of California, Berkeley under an Office of Naval Research grant no. N00014-03-C-0187, SPO no. 016671-004, and a Berkeley Fellowship. The authors would also like to thank Stephen Spry for his help with the optimal control analysis.

References

[1] McGee, T., Spry, S., and Hedrick, J. K., "Optimal Path Planning in a Constant Wind with a Bounded Turning Rate," AIAA Paper 2005-6186, 2005.

[2] Dubins, L., "On Curves of Minimal Length with a Constraint on Average Curvature, and with Prescribed Initial and Terminal Positions and Tangents," *American Journal of Mathematics*, Vol. 79, No. 3, 1957, pp. 497–516.

[3] Reeds, J. A., and Shepp, L. A., "Optimal Paths for a Car that Goes Both Forward and Backwards," *Pacific Journal of Mathematics*, Vol. 145,

No. 2, 1990, pp. 367–393.

[4] Boissonnat, J. D., Cerezo, A., and Leblond, J., "Shortest Paths of Bounded Curvature in the Plane," *Journal of Intelligent and Robotic Systems: Theory and Applications*, Vol. 11, No. 1–2, 1994, pp. 5–20.

[5] Tang, Z., and Ozguner, U., "Motion Planning for Multitarget Surveillance with Mobile Sensor Agents," *IEEE Transactions on Robotics and Automation*, Vol. 21, No. 5, 2005, pp. 898–908.

[6] Yang, G., and Kapila, V., "Optimal Path Planning for Unmanned Air Vehicles with Kinematic and Tactical Constraints," IEEE Paper 0-7803-7516-5/02, 2002, pp. 1301–1306.

[7] Agarwal, P. K., Raghavan, P., and Tamakai, H., "Motion Planning for a Steering-Constrained Robot Through Moderate Obstacles," ACM Paper 0-89791-718-9/95/0005, 1995, pp. 343–352.

[8] Bicchi, A., Canaline, G., and Santiago, C., "Planning Shortest Bounded-Curvature Paths for a Class of Nonholonomic Vehicles Among Obstacles," *Journal of Intelligent and Robotic Systems: Theory and Applications*, Vol. 16, No. 4, 1996, pp. 387–405.

[9] Bryson, A., and Ho, Y. C., *Applied Optimal Control: Optimization, Estimation, and Control*, John Wiley and Sons, New York, 1975.

[10] Croft, E., Fenton, R., and Benhabib, B., "Optimal Rendezvous-point Selection for Robotic Interception of Moving Objects," *IEEE Transactions on Systems, Man, and Cybernetics, Part B: Cybernetics*, Vol. 28, No. 2, 1998, pp. 192–204.

[11] Bui, X. N., Boissonnat, J. D., Soueres, P., and Laumond, J. P., "Shortest Path Synthesis for Dubins Non-Holonomic Robot," IEEE Paper 1050-4729/94, 1994, pp. 2–7.

[12] McGee, T. G., and Hedrick, J. K., "Path Planning and Control for Multiple Point Surveillance by an Unmanned Aircraft in Wind," IEEE Paper 0-7803-8914-X/05, 2006, pp. 4261–4266.